



Accepted Article

Title: Synthesis, Structure, Biological Evaluation and Catalysis of Two Pyrazole-Functionalized NHC-Ru(II) Complexes

Authors: Chao Chen; Shengliang Ni; Qing Zheng; Meifang Yu; Hangxiang Wang

This manuscript has been accepted after peer review and the authors have elected to post their Accepted Article online prior to editing, proofing, and formal publication of the final Version of Record (VoR). This work is currently citable by using the Digital Object Identifier (DOI) given below. The VoR will be published online in Early View as soon as possible and may be different to this Accepted Article as a result of editing. Readers should obtain the VoR from the journal website shown below when it is published to ensure accuracy of information. The authors are responsible for the content of this Accepted Article.

To be cited as: Eur. J. Inorg. Chem. 10.1002/ejic.201601116

Link to VoR: <https://doi.org/10.1002/ejic.201601116>

Synthesis, Structure, Biological Evaluation and Catalysis of Two Pyrazole-Functionalized NHC-Ru(II) Complexes

Chao Chen,^{*,[a]} Shengliang Ni,^[a] Qing Zheng,^[a] Meifang Yu,^[a] and Hangxiang Wang^{*,[b]}

Abstract: Two ruthenium complexes bearing pyrazole-functionalized N-heterocyclic carbenes (NHCs) (**3a** and **3b**) were prepared and their structures were characterized by X-ray diffraction analysis. Owing to the promising anticancer potential, we evaluated the cytotoxicity of both complexes against a panel of human cancer cell lines, including breast cancer Bcap-37, colorectal cancer LoVo, gastric cancer SCG7901, and cisplatin-resistant SCG7901-R cells. *In vitro* results showed that complex **3a** inhibited cancer cell proliferation, which was comparable cytotoxicity with clinically approved cisplatin. More impressively, complex **3a** evoked significant death of cisplatin-resistant gastric cancer SCG7901-R cells, displaying a approximately 13-fold lower IC₅₀ value in this type of cells than cisplatin (i.e., 5.8 ± 0.4 μM versus 83.1 ± 14.5 μM). Collectively, these results highlighted the potential utility using ruthenium-NHC complexes as highly efficient catalysts as well as promising candidates for treating cancers that are resistant to platinum-based therapy. In addition, both ruthenium-NHC complexes were demonstrated to be efficient catalysts for the oxidation of various alcohols. Exploiting them as catalysts, a variety of carbonyl products were obtained in excellent yields.

Introduction

N-Heterocyclic carbenes (NHCs) are known as versatile ligands in classical and modern chemistry with the properties of strong σ-donating ability, steric and electronic tunable effects, and ease of preparation.^[1] Among NHCs, the functionalized-NHC with reversible donor groups show great advantages in homogeneous reactions and in obtaining coordination complexes because they would allow a further fine-tuning of the metal environment in obtaining sophisticated complexes.^[2] Functionalized-NHC complexes incorporating phosphine, nitrogen, oxygen, and sulfur groups have been achieved and shown wide application in transformations such as cross-coupling, transfer hydrogenation, hydrogenation, and polymerization.^[3-6]

On the other hand, metal-containing complexes have attracted considerable attention because of their promising therapeutic potential as anticancer drugs.^[7] As a pioneering example, cisplatin [*cis*-dichlorodiamineplatinum(II)] was approved for the

of significant dose-limiting toxicities and acquired or intrinsic drug resistance.^[8] Therefore, exploration of novel metallodrugs that can circumvent these drawbacks is desperately needed. Within this field, among ligands, probably the metallodrugs supported by functionalized-NHC remains the great potential in application. Functionalized-NHC complexes, including Ag, Au, Pt, Pd, Cu, Ni, and Ru have displayed promising pharmacological characteristics as anticancer agents, and many of them have shown high therapeutic potency.^[9] These non-platinum complexes targeted distinct pathways and exhibited different modes of action to evoke the death of cancer cells compared with platinum drugs.^[10] Thus, this novel metal complexes could be therapeutically potential to mitigate the side effects induced by platinum drugs and effectively treat cancer types that are resistant to platinum-based therapy.

Previously, we reported that nickel, palladium, platinum, and ruthenium complexes containing pyridine-, pyrimidine-, and pyrazole-functionalized NHC ligands exhibited intriguing structures and enhanced catalytic activities in homogeneous reactions.^[11] However, the biological activities of these complexes have never been investigated. As a part of our ongoing work, here we report the synthesis and structural characterization of two novel pyrazole-functionalized NHC-ruthenium complexes, [RuCl(L1)(*p*-cymene)](PF₆) (**3a**) (L1 = 1-ethyl-3-(*N*-mesitylimidazolylidene)methyl)-5-methyl-pyrazole) and [Ru₂Cl₂(L2)(*p*-cymene)₂](PF₆)₂ (**3b**) (L2 = 3,6-di((1-ethyl-5-methyl-pyrazol-3-yl)methyl)-1-imidazolylidene)pyridazine). The respective *in vitro* anticancer cytotoxicity against a panel of human cancer cell lines was evaluated. Additionally, the catalytic activity of two ruthenium-NHC complexes in the oxidation of alcohols was demonstrated using structurally distinct substrates.

Results and Discussion

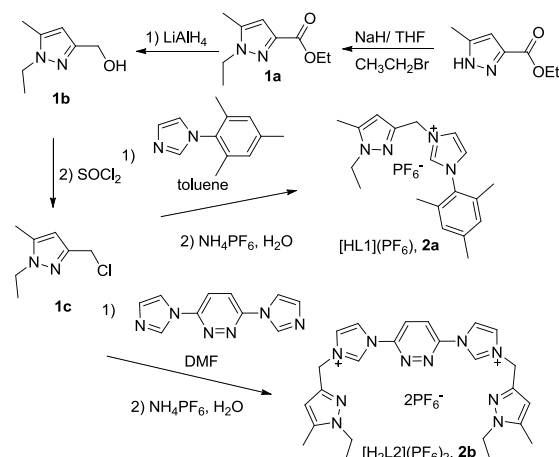
The synthetic routes for the NHC ligand precursors are illustrated in Scheme 1. 1,3-(chloromethyl)-1-ethyl-5-methyl-pyrazole (**1c**) was synthesized starting from ethyl 5-methyl-pyrazole-3-carboxylate. The imidazolium salt 1-ethyl-3-(*N*-mesitylimidazoliummethyl)-5-methyl-pyrazole hexafluorophosphate (**2a**) ([HL1](PF₆)) was readily obtained by reacting **1c** with *N*-mesitylimidazole in refluxing toluene and subsequent anion exchange reaction with NH₄PF₆ in water. However, when we followed the same procedure as used for [HL1](PF₆) (**2a**), the reaction of **1c** with 3,6-di(1H-imidazol-1-yl)pyridazine in refluxing toluene yielded crude products that cannot be isolated. Therefore, we attempted the preparation of imidazolium salt 3,6-di((1-ethyl-5-methyl-pyrazol-3-yl)methyl)-1-imidazolium)pyridazine dihexafluorophosphate (**2b**) ([H₂L2](PF₆)₂) in hot DMF solvent followed by anion exchange in water. Both of the imidazolium salts were characterized by NMR spectroscopy and elemental analysis. The formation of two imidazolium salts were evidenced by the presence of the downfield resonance signals at 9.46 and 10.40 ppm for

[a] College of Life Sciences, Huzhou University, East 2nd Road, Huzhou, 313000, China
E-mail: chenc@zjhu.edu.cn

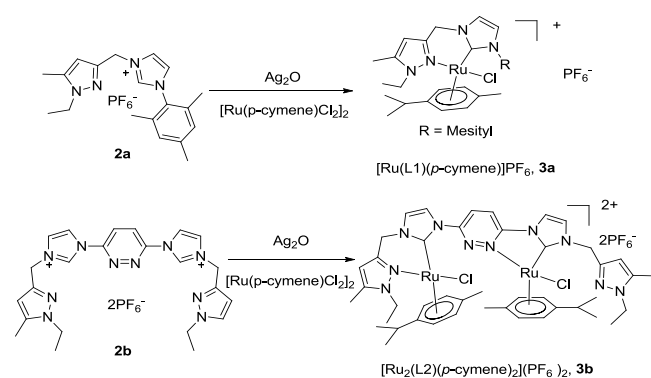
[b] The First Affiliated Hospital, School of Medicine, Zhejiang University, Hangzhou, 310003, China.
E-mail: wanghx@zju.edu.cn
Supporting information for this article is given via a link at the end of the document.

clinical use by the end of 1970s. However, it must be pointed out that platinum-based anticancer drugs pose challenges because

[HL1](PF₆) (**2a**) and [H₂L2](PF₆)₂ (**2b**), respectively, due to the acidic imidazolium protons in ¹H NMR spectra. The signals at 8.00, 7.91, 6.13 and 5.43 ppm for [HL1](PF₆) and 8.65, 8.10, 6.25 and 5.52 ppm for [H₂L2](PF₆)₂ could be assigned to the imidazolylidene backbone, pyrazole CH and methylene protons, respectively.



Scheme 1. Synthesis of [HL1](PF₆) (**2a**) and [H₂L2](PF₆)₂ (**2b**).



Scheme 2. Synthesis of [Ru(L1)(p-cymene)](PF₆) (**3a**) and [Ru₂(L2)(p-cymene)₂](PF₆)₂ (**3b**).

The final adducts, ruthenium–NHC complexes [RuCl(L1)(p-cymene)](PF₆) (**3a**) and [Ru₂Cl₂(L2)(p-cymene)₂](PF₆)₂ (**3b**), were synthesized by the conventional carbene-transfer reaction by stirring the *in situ* generated Ag–NHC complexes with [Ru(p-cymene)Cl₂]₂ in acetonitrile (Scheme 2). Ultimately, these two NHC–ruthenium complexes were isolated as air- and moisture-stable solids after crystallization in acetonitrile/ether. The formulation of **3a** and **3b** were firstly characterized by NMR spectroscopy. In their ¹H NMR, the absence of peaks around 10 ppm ascribed to acidic NCHN imiazolium protons supported the coordination of the carbene ligand. ¹H NMR spectra of **3a** and **3b** also indicated characteristic peaks ascribed to p-cymene groups and NHC ligands. In complex **3a**, three singlet signals at

7.54, 7.16, and 6.36 ppm were observed due to the imidazolylidene backbone and pyrazole CH protons, whereas two doublets at 5.31 and 4.96 ppm were assigned to the methylene protons. The p-cymene signals of **3a** resonated at 5.34–5.86 ppm which was similar to those of the known NHC–Ru-(p-cymene) complexes depending on the ancillary ligands.^[12] In addition, ¹³C NMR spectra of **3a** exhibited carbenic carbon resonances at 173.8 ppm which was a typical peak of ruthenium-carbene complex. In both ¹H and ¹³C spectra of **3b**, two set of resonance signals assigned to the ligand has been observed, illustrating that the symmetrical ligands become inequivalent. Obviously, the resonances due to the methylene protons appeared as four doublets at 5.54, 5.49, 5.41, and 4.99 ppm. ¹³C NMR spectrum of complex **3b** exhibited two singlets at 187.5 and 177.7 ppm, characteristic of two carbenic carbons.

The solid structure detail of complex **3a** was depicted in Figure 1. The center Ru(II) ion in complex **3a** was hexacoordinated by one didentate NHC ligand, one chloride and one η⁶-coordinated p-cymene group in a usual piano-stool geometry, with one carbon atom of imidazolylidene, one nitrogen atom of pyrazole, and one chloride as legs. The angles between the piano legs, C–Ru–N (83.88°), N–Ru–Cl (88.31°), Cl–Ru–C (87.97°) were ranged within the excepted bond angles compared with other similar ruthenium complexes. The η⁶-coordinated benzene ring of the p-cymene group was almost planar and the center Ru(II) ion was 1.712 Å out of the centroid of the benzene ring. The Ru–C distance (2.079 Å), Ru–N distance (2.122 Å) and Ru–Cl distance (2.389 Å) were also consistent with the reported values in known NHC–Ru-(p-cymene) complexes.^[13]

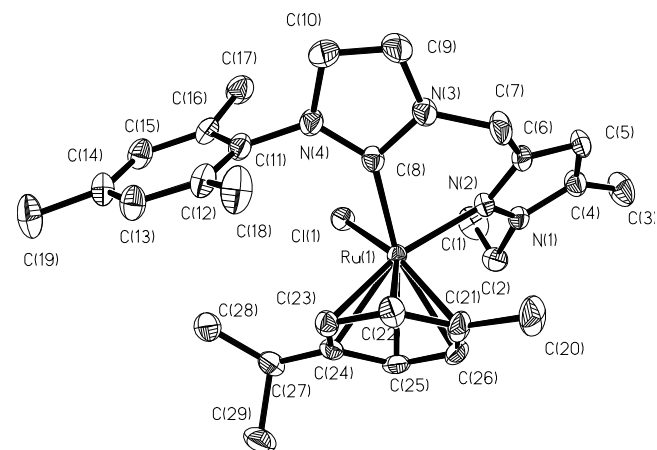


Figure 1. X-ray diffraction structures of Ru–NHC complex **3a**.

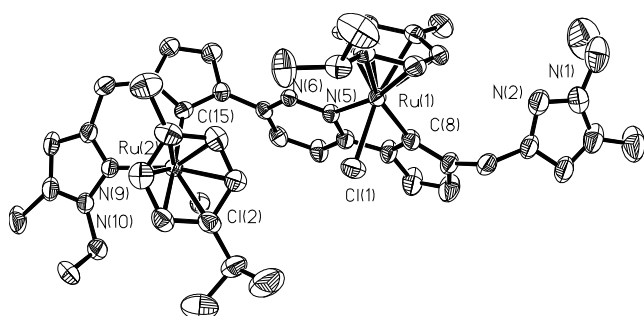


Figure 2. X-ray diffraction structures of Ru-NHC complex **3b**.

The cationic structure of **3b** was shown in Figure 2. X-ray analysis revealed that **3b** consisted of one pyrazole and pyridazine co-functionalized NHC ligand (L2), two discrete Ru(II) ions and two *p*-cymene groups. Both Ru(II) ions were hexa-coordinated by C, N, Cl atoms and *p*-cymene group, and also displayed a typical piano-stool geometry. However, one Ru(II) ion was coordinated by a pyrazole nitrogen atom and the other Ru(II) ion was coordinated by a pyridazine nitrogen atom. The different coordinated nitrogen atoms of two Ru(II) atoms led to form an asymmetrical structure of **3b**. In L2 moiety, two imidazolylidene rings were almost perpendicular to each other with a dihedral angle of 87.81° and one imidazolylidene ring was parallel to the pyridazine plane with a dihedral angle of 11.57°, the other imidazolylidene ring was perpendicular to the pyridazine plane with a dihedral angle of 89.15°. The angles between piano legs (e.g., C(8)-Ru(1)-N(5) = 76.47°, N(5)-Ru(1)-Cl(1) = 86.81°, Cl(1)-Ru(1)-C(8) = 83.84°, C(15)-Ru(2)-N(9) = 84.66°, N(9)-Ru(2)-Cl(2) = 85.98°, and Cl(2)-Ru(2)-C(15) = 85.55°) were comparable with complex **3a**. The distances for Ru-C(carbene), Ru-N, and Ru-Cl ranged from 2.008 to 2.048 Å, 2.086 to 2.143 Å, and 2.390 to 2.394 Å, respectively, and also were comparable with those of hexa-coordinated Ru(II) complexes bearing NHC ligands.^[13] The separation between Ru...Ru was relatively long (6.384 Å), thus excluding any metal-metal interaction. In previous reports, dinuclear complexes of pyridazine-functionalized NHCs such as [Ru₂Cl(L)(CH₃CN)₄](PF₆)₃, [Pd₂(allyl)₂L] (L = 3,6-bis-(N-(pyridylmethyl)imidazolylidene)pyridazine),^[14] [Hg₂(3,6-bis(1-methylimidazol-2-ylidyl)pyridine)₂](PF₆)₄,^[15] [Ag₂(3,6-bis(1-*n*-butylimidazol-2-ylidyl)pyridine)₂][AgCl₂]₂,^[16] are usually symmetrical. However, complex **3b** represent an rare example of unsymmetrical dinuclear complex coordinated by pyridazine bridged NHC ligand.^[17]

Ruthenium complexes are a class of therapeutically potential candidates, serving as non-platinum metal anticancer agents. Upon administration *in vivo*, ruthenium complexes are expected to exhibit attractive features such as low systemic toxicity and feasibility for absorption in body. More importantly, they are likely to overcome the drug resistance induced by platinum compounds.^[18] Consequently, two ruthenium-based complexes (i.e., NAMI-A and KP1019) have entered clinical trials.^[19]

To evaluate the potential using these novel Ru-NHCs as anticancer drugs, *in vitro* cytotoxicity of complexes **3a** and **3b** were assessed by MTT assay against four different human cancer cell lines, including breast cancer Bcap-37, colon cancer LoVo, gastric cancer SCG7901, and cisplatin-resistant gastric cancer SCG7901-R cells.^[20] Cisplatin was included as control. As indicated in Figure 3 and Table 1, it was concluded that

complex **3a** possessed the comparable or even superior cytotoxicity compared with cisplatin across different non-resistance cell types. For example, the half maximal inhibitory concentration (IC₅₀) values of complex **3a** were 11.2 ± 0.8, 9.2 ± 0.5, and 2.9 ± 0.5 μM in Bcap-37, LoVo, and SCG7901 cells, respectively, whereas the IC₅₀ values for cisplatin were 8.5 ± 0.9, 4.1 ± 0.2, and 10.5 ± 0.6 μM in above three types of cells, respectively. By sharp contrast, complex **3b** bearing the same NHC-Ru(*p*-cymene) core was less efficacious than either complex **3a** or cisplatin in all tested cancer cells. The enhanced cytotoxicity activity of complex **3a** may attribute to the high lipophilicity substitution of mesityl at the position of imidazolylidene ring promoting cellular uptake.^[21] Several other Ru-NHCs including Grubbs catalysts have been evaluated for their anticancer properties.^[22] However, the anticancer activities of Ru-NHC complexes against cisplatin-resistant cancer cells

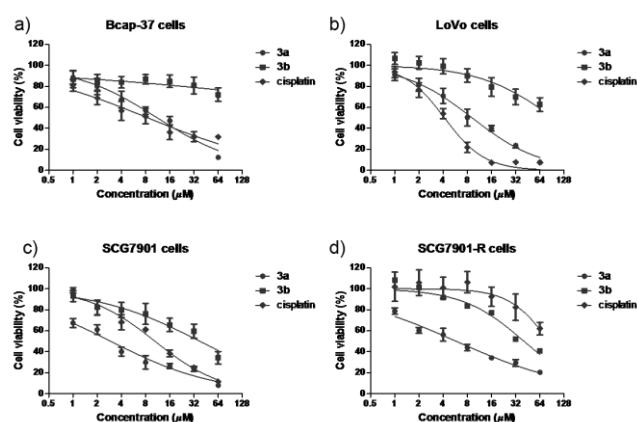


Figure 3. The cell viability of Bcap-37, LoVo, SCG7901, and SCG7901-R cells after 48-h treatment with complex **3a** and **3b**, and cisplatin as determined by MTT assay. The data were expressed as the means ± SD (n = 4).

Table 1. IC₅₀ values of complex **3a**, **3b**, and cisplatin against various cancer cell lines after 48h drug exposure.

Cell line	Cell type	IC ₅₀ (μM) ^[a]		
		3a	3b	Cisplatin
Bcap-37	Breast	11.2±0.8	>100	8.5±0.9
LoVo	Colorectal	9.2±0.5	94.2±18.9	4.1±0.2
SCG7901	Gastric	2.9±0.5	37.7±5.3	10.5±0.6
SCG7901-R	Cisplatin-resistant	5.8±0.4	40.6±3.8	83.1±14.5
Ratio of SCG7901-R/SCG7901		2.0	-	7.9

[a] IC₅₀ values were determined by MTT assay.

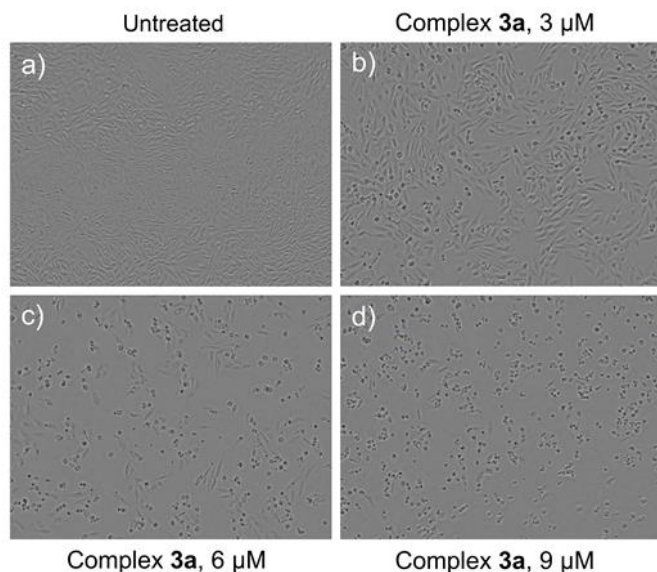


Figure 4. Morphology changes of LoVo cells upon treating with complex **3a** at 3, 6 and 9 μM . After 48-h incubation of **3a**, the cells were photographed by microscope (magnification 100 \times).

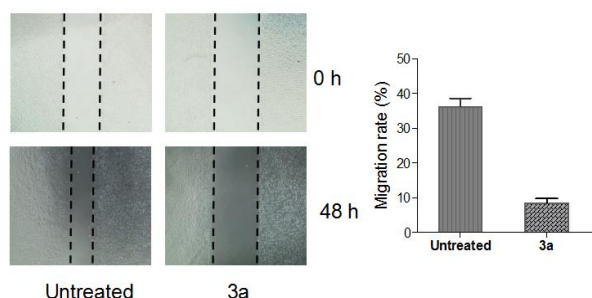


Figure 5. Graphs of scratch-wound healing assay using LoVo cells in the absence or presence of **3a** of 4 μM . After 48h incubation, migration rates were calculated from migration areas. The cells were photographed by microscope (magnification 40 \times).

have not been studied so far. These results prompted us to further investigate their efficacy in cisplatin-resistant cancer cells (i.e., gastric cancer SCG7901-R cells). Surprisingly, we found that complex **3a** substantially induced cisplatin-resistant SCG7901-R cells kill with low IC_{50} value occurred at $5.8 \pm 0.4 \mu\text{M}$, which was approximately 13-fold lower IC_{50} value than cisplatin ($83.1 \pm 0.4 \mu\text{M}$). Several cellular processes are involved in cancer drug resistance toward cisplatin, including low expression of the copper transport protein (Ctr1), enhanced presence of glutathione system, and improved DNA repair pathways.^[23] Unfortunately, these factor-associated drug resistance were difficult to be overcome by the use of classical platinum-based complexes. Therefore, Ru-NHC complexes presented here may be promising against cancer types that are resistant to platinum-based therapy.

To further confirm the biological activity of complex **3a**, we investigated the ability of complex **3a** to induce the morphology changes in LoVo cells. As shown in Figure 4, the treatment of complex **3a** with increased concentrations (e.g., 3, 6 and 9 μM) dramatically decreased the density of LoVo cells. Specifically, complex **3a** almost killed all of the cells at 9 μM . This result provided the direct evidence that complex **3a** could efficiently inhibit the proliferation of cancer cells and destroy cancer cells. Moreover, the cells exhibited shrinkage and turned to be round. This indicated that complex **3a** can induce the apoptosis of the cancer cells.^[21] Finally, scratch-wound cell migration assay of LoVo cells was tested (Figure 5). The results showed that the migration of LoVo cells was suppressed by complex **3a**. The migration proportion of the untreated cells was 36% after 48-h incubation, whereas the percentage of migration was reduced to 8.5% upon treating with complex **3a** (4 μM) after 48 h.

In addition to displaying promising biological activity, the Ru-NHC complexes **3a** and **3b** presented here contained strong Ru-carbene bond and reversible de-coordination and coordination nitrogen heterocyclic group, we envisaged that they should be good catalyst candidates.^[24,12b] Therefore, the catalytic activity of **3a** and **3b** for the oxidation of alcohol derivatives was investigated. To optimize the reaction conditions, benzyl alcohol was first selected as a model substrate to evaluate the catalytic activity of complexes **3a** and **3b**. To avoid the formation of byproducts at high temperature, we tested this reaction at relatively low temperature in the presence of oxidant but without base. To our delight, in the presence of hydrogen peroxide (H_2O_2) at 60 $^\circ\text{C}$, complexes **3a** and **3b** were fairly efficient, affording benzaldehyde in excellent yields within 2 h in acetonitrile. In contrast, only trace amount of the product was observed in the absence of the catalysts (see table S1).

Encouraged by these results, we thus explored the oxidation of a wide range of alcohol derivatives, including substituted primary and secondary alcohols. The reactions were performed in the presence of Ru-NHCs and H_2O_2 at 60 $^\circ\text{C}$ in acetonitrile. Complexes **3a** and **3b** were found to be highly active in oxidation of structurally diverse substrates. For instance, both electron-withdrawing and electron-donating benzyl alcohols were converted to the corresponding products in excellent yields within 2 h. Sterically hindered ortho-substituted substrates such as 2-methoxyphenylmethanol, 2-bromophenylmethanol and 2-nitrophenylmethanol were also easily converted to corresponding carbonyl complexes after 3h reaction. It is worth to note that heterocyclic alcohols, 2-thiophenmethanol and 3-pyridinemethanol, were also efficiently oxidized with an increased reaction time of 5 h, indicating that both ruthenium complexes exhibited high tolerance. In addition, the catalysts were also suitable for oxidation of secondary alcohols, and the target products could be obtained in good to excellent yields (see table S2).

Conclusions

In summary, we have reported the preparation of two pyrazole-functionalized ruthenium-NHC complexes, and their structures

were identified by X-ray diffraction analysis. Results from the cytotoxicity studies clearly demonstrated that Ru-NHC complex **3a** possessed promising anticancer efficacy across different cell types. Most intriguingly, complex **3a** showed high potency for evoking significant death in cancer cells that are resistant to the cisplatin agent, providing a clue to the development of a new class of chemotherapeutics for cancer therapy. Owing to their therapeutic potential to treat those chemoresistant malignancies, further work will be conducted to understand the correlation between the structures of NHC ligands and anticancer activity as well as the molecular mechanisms underlying the death of cancer cells. Additionally, both of Ru-NHCs complexes showed high catalytic potency for the oxidation of structurally diverse alcohol derivatives.

Experimental Section

All chemicals were of reagent grade quality obtained from commercial sources and used as received, unless stated otherwise. 5-methylpyrazole-3-carboxylate was synthesized according to the literature method.^[25] ¹H and ¹³C NMR spectra were recorded on a Bruker Avance-400 (400 MHz) spectrometer 400 MHz for ¹H and 100 MHz for ¹³C. Chemical shifts (δ) are expressed in ppm downfield to TMS at $\delta = 0$ ppm and coupling constants (J) are expressed in Hz. Elemental analyses were performed by Flash EA 1112 Thermo Finnigan.

Synthesis of ethyl 1-ethyl-5-methyl-pyrazole-3-carboxylate (1a). A solution of ethyl 5-methyl-pyrazole-3-carboxylate (23.1 g, 0.15 mol) in dry THF (300 mL) was slowly treated with NaH (4.3 g, 0.18 mol). The mixture was stirred for 30 min until hydrogen evolution ceased. CH₃CH₂Br (19.4 g, 0.18 mol) dissolved in dry THF (50 mL) was added dropwise and the resulting mixture was stirred for 6 h at room temperature. The solvent was evaporated and an aqueous solution of NaHCO₃ was added to the residue. The mixture was extracted three times with CH₂Cl₂ (3 x 100 mL), the organic phases were combined, dried with Na₂SO₄, and the solvent was evaporated to give a yellow liquid. Yield: 24.6 g, 90%. ¹H NMR (CDCl₃): 6.47 (s, pyrazole CH, 1H), 4.31 (q, CH₂CH₃, $J = 7.2$ Hz, 2H), 4.10 (q, CH₂CH₃, $J = 7.2$ Hz, 2H), 2.24 (s, CH₃, 3H), 1.35 (t, CH₂CH₃, $J = 7.2$ Hz, 3H), 1.31 (t, CH₂CH₃, $J = 7.2$ Hz, 3H). ¹³C NMR (CDCl₃): 162.5, 142.0, 138.9, 108.2, 60.5, 44.6, 15.1, 14.3, 10.8. HRMS (TOF MS EI⁺) m/z calcd for C₉H₁₄N₂O₂, 182.1055; found 182.1060.

Synthesis of 3-(hydroxymethyl)-1-ethyl-5-methyl-pyrazole (1b). A solution of ethyl 1-ethyl-5-methyl-pyrazole-3-carboxylate (18.2, 0.1 mol) in 100 mL dry THF was added to a suspension of LiAlH₄ (7.6, 0.2 mol) in 300 mL dry THF at room temperature. The suspension was stirred for 4 h at room temperature. Then, the suspension was cautiously quenched by addition of C₂H₅OH (50 mL). The solvent was removed under reduced pressure, and the resulting white solid was suspended in methanol (500 mL). The suspension was neutralized with concentrated HCl and refluxed for 6 h. The solid was filtered, and the filtrate was evaporated to give an oily residue. Then the residue was dissolved in CH₂Cl₂ and filtered. The filtrate was dried over Na₂SO₄, concentrated under reduced pressure to give a yellow liquid. Yield: 10.9 g, 78%. ¹H NMR (CDCl₃): 5.75 (br+s, pyrazole CH and CH₂OH, 2H), 4.52 (s, CH₂, 2H), 3.86 (q, CH₂CH₃, $J = 7.2$ Hz, 2H), 2.07 (s, CH₃, 3H), 1.13 (t, CH₂CH₃, $J = 7.2$ Hz, 3H). ¹³C NMR (CDCl₃): 150.7, 139.1, 103.5, 58.1, 43.6, 15.3, 11.0. HRMS (TOF MS EI⁺) m/z calcd for C₇H₁₂N₂O, 140.0950; found 140.0952.

Synthesis of 3-(chloromethyl)-1-ethyl-5-methyl-pyrazole (1c). Thionyl chloride (5 mL, 68 mmol) was slowly added to a solution of **1b** (7.0 g, 50 mol) in CH₂Cl₂ (50 mL) at RT. The reaction mixture was stirred for 2 h, then the reaction mixture was poured into an ice-cold solution of saturated aqueous NaHCO₃ (50 mL) and CH₂Cl₂ (50 mL). The phases were separated and the aqueous phase was extracted with CH₂Cl₂ (2 x 50 mL). The combined organic phases were washed with water (50 mL), dried over Na₂SO₄ and concentrated under reduced pressure to give **1c** as a yellow liquid. Yield: 7.6 g, 96%. ¹H NMR (CDCl₃): 6.06 (s, pyrazole CH, 1H), 4.55 (s, CH₂, 2H), 4.03 (q, CH₂CH₃, $J = 7.2$ Hz, 2H), 2.25 (s, CH₃, 3H), 1.38 (t, CH₂CH₃, $J = 7.2$ Hz, 3H). ¹³C NMR (CDCl₃): 147.3, 138.9, 104.8, 43.9, 39.3, 15.3, 11.0. HRMS (TOF MS EI⁺) m/z calcd for C₇H₁₁N₂Cl, 158.0611; found 158.0612.

Synthesis of 1-ethyl-3-(N-mesitylimidazolium)methyl-5-methyl-pyrazole hexafluorophosphate ([HL1](PF₆)) (2a). A solution of **1c** (1.58 g, 10 mmol) and *N*-methylimidazole (1.86 g, 10 mmol) in toluene (10 mL) was refluxed overnight. The resulting solid was dissolved in water and then a saturated NH₄PF₆ aqueous solution (10 mL) was added dropwise. The resulting white precipitate was filtered and washed with water, ethanol, and ether. Yield: 3.76 g, 83%. Anal. Calcd for C₁₉H₂₅F₆N₄P: C, 49.93; H, 6.19; N, 13.23. Found: C, 49.86; H, 6.16; N, 13.31. ¹H NMR (400 MHz, DMSO-*d*₆): δ 9.46 (s, NCHN, 1H), 8.00, 7.91 (both s, NCHCHN, each 1H), 7.15 (s, Mesityl CH, 2H), 6.13 (s, pyrazole CH, 1H), 5.43 (s, CH₂, 2H), 4.02 (q, CH₂CH₃, $J = 7.2$ Hz, 2H), 2.33 (s, Mesityl CH₃, 3H), 2.26 (s, CH₃, 3H), 2.01 (s, Mesityl CH₃, 6H), 1.27 (t, CH₂CH₃, $J = 7.2$ Hz, 3H). ¹³C NMR (100 MHz, DMSO-*d*₆): δ 144.1, 140.7, 139.9, 138.2, 134.7, 131.6, 129.7, 124.4, 123.9, 124.4, 123.9, 104.5, 47.4, 43.8, 21.0, 17.3, 15.5, 11.0.

Synthesis of 3,6-di(3-((1-ethyl-5-methyl-pyrazol-3-yl)methyl)-1-imidazolium)pyridazine dihexafluorophosphate, ([H₂L2](PF₆)₂) (2b). A solution of 3,6-di(imidazol-1-yl)pyridazine (2.12 g, 10 mmol) and **1c** (4.74 g, 30 mmol) in 20 mL of DMF was stirred at 100 °C overnight. The resulting white solid was collected by filtration and dissolved in 100 mL of water. Subsequent addition of saturated NH₄PF₆ to the aqueous solution afforded a white precipitate, which was collected by filtration and dried. Yield: 2.15 g, 48%. Anal. Calcd for C₂₄H₃₀F₁₂N₁₀P₂: C, 38.51; H, 4.04; N, 18.71. Found: C, 38.43; H, 3.91; N, 18.62. ¹H NMR (400 MHz, DMSO-*d*₆): δ 10.40 (s, NCHN, 2H), 8.80 (s, pyridazine CH, 2H), 8.65, 8.10 (both s, NCHCHN, each 2H), 6.25 (s, pyrazole CH, 2H), 5.52 (s, CH₂, 4H), 4.06 (q, CH₂CH₃, $J = 7.2$ Hz, 4H), 2.27 (s, CH₃, 6H), 1.31 (t, CH₂CH₃, $J = 7.2$ Hz, 6H). ¹³C NMR (100 MHz, DMSO-*d*₆): δ 152.0, 143.5, 139.9, 136.3, 124.5, 124.0, 120.6, 105.3, 47.7, 43.9, 15.6, 10.9.

Synthesis of [RuCl(L1)(*p*-cymene)](PF₆), **3a.** A mixture of **2a** (454 mg, 1.0 mmol), Ag₂O (116 mg, 0.5 mmol) in 10 mL CH₃CN was stirred at 50 °C for 4 h. After it was cooled to room temperature, [Ru(*p*-cymene)Cl₂]₂ (306 mg, 0.50 mmol) was added to the solution and stirred at room temperature for another 2 h. Then the mixture was filtered through Celite, and all volatiles were evaporated under reduced pressure. The yellow residue was dissolved in CH₃CN and crystallization by slow diffusion of Et₂O into the CH₃CN solution gave **3a** as yellow solid, 333 mg, 46%. Anal. Calcd for C₂₉H₃₈ClF₆N₄PRu: C, 48.10; H, 5.29; N, 7.74. Found: C, 47.88; H, 5.06; N, 7.83. ¹H NMR (CD₃CN): 7.54 (s, imidazole CH, 1H), 7.16 (s, imidazole CH, 1H), 7.14 (s, Mes CH, 1H), 6.99 (s, Mes CH, 1H), 6.36 (s, pyrazole CH, 1H), 5.86, 5.78, 5.43, 5.34 (both d, $J = 6.0$ Hz, *p*-cymene CH, 4H), 5.31, 4.96 (both d, $J = 16.0$ Hz, CH₂, 2H), 4.86-4.69 (m, CH₃CH₂, 2H), 2.48 (s, Mes CH₃, 3H), 2.36 (s, Mes CH₃, 3H), 2.25 (s, Mes CH₃, 3H), 2.02 (s, *p*-cymene CH₃, 3H), 1.98-1.96 (m, *p*-cymene CH(CH₃)₂, 1H), 1.60 (s, pyrazole CH₃, 3H), 1.40 (t, $J = 7.2$ Hz, CH₃CH₂, 3H), 1.14, 0.58 (both d, $J = 6.8$ Hz, *p*-cymene CH(CH₃)₂, 6H). ¹³C NMR (CD₃CN): 173.8 (Ru-C), 146.8, 146.3, 146.1, 140.1, 138.7,

136.5, 136.4, 129.9, 128.8, 126.2, 124.2, 107.4, 89.5, 87.5, 47.8, 46.1, 31.5, 23.9, 20.7, 19.7, 19.6, 18.0, 17.9, 15.4, 12.2

Synthesis of $[Ru_2Cl_2(L2)(p\text{-cymene})_2](PF_6)_2$, **3b.** Complex **3b** was prepared similarly as for **3a** and isolated as a yellow solid. Yield: 387 mg, 30%. Anal. Calcd for $C_{44}H_{56}Cl_2F_{12}N_{10}P_2Ru_2$: C, 41.03; H, 4.38; N, 10.88. Found: C, 41.28; H, 4.65; N, 10.83. 1H NMR (CD_3CN): 8.20, 8.12 (both d, pyridazine CH, $J = 9.2$ Hz, 2H), 7.98, 7.66, 7.63, 7.57 (both d, imidazole CH, $J = 2.4$ Hz, 4H), 6.44, 6.24, 6.07, 5.93, 5.80, 5.34, 5.15 (both d, $J = 6.0$ Hz, *p*-cymene CH, 8H), 6.37, 6.26 (both s, pyrazole CH, 2H), 5.54, 5.49 (both d, CH_2 , $J = 15.2$ Hz, 2H), 5.41, 4.99 (both d, CH_2 , $J = 16.0$ Hz, 2H), 4.71-5.65, 4.51-4.46 (both m, CH_3CH_2 , 2H), 3.43 (q, $J = 7.2$ Hz, CH_3CH_2 , 2H), 2.66-2.59 (m, *p*-cymene $CH(CH_3)_2$, H), 2.45-2.43 (m+s, *p*-cymene $CH(CH_3)_2$ and CH_3 , 4H), 2.33 (s, *p*-cymene CH_3 , 3H), 2.14, 2.12 (both s, pyrazole CH_3 , 6H), 1.39, 1.34 (t, $J = 7.2$ Hz, CH_3CH_2 , 6H), 1.18-1.11 (m, *p*-cymene $CH(CH_3)_2$, 6H), 0.97, 0.91 (both d, $J = 6.8$ Hz, *p*-cymene $CH(CH_3)_2$, 6H). ^{13}C NMR (CD_3CN): 187.5 (Ru-C), 177.7 (Ru-C), 155.9, 154.5, 147.0, 145.8, 145.4, 140.7, 134.2, 126.1, 125.7, 124.4, 120.2, 118.6, 113.3, 110.0, 108.1, 107.6, 105.4, 103.6, 93.0, 92.3, 90.9, 89.2, 85.8, 85.7, 85.3, 83.3, 49.5, 47.6, 45.8, 44.4, 32.0, 31.4, 24.2, 22.4, 22.1, 20.6, 19.0, 18.5, 15.3, 12.0, 10.7.

Cell cytotoxicity assay. The cytotoxicity of complexes **3a**, **3b**, and cisplatin against human cancer cell lines (breast cancer Bcap-37, colorectal cancer LoVo, gastric cancer SCG7901, and cisplatin-resistant SCG7901-R) was determined using MTT assay. The cells were plated in 96-well plates (5000 cells per well) and incubated at 37°C for 24 h. Dilutions of complexes **3a**, **3b** and cisplatin in DMSO were added to the cells, and the cells were further incubated for 48 h. Subsequently, 30 μ L of MTT solution (5 mg/mL) was added to each well. The plates were incubated at 37 °C for 4 h, allowing viable cells to reduce the yellow tetrazolium salt into dark blue formazan crystals. After the addition of DMSO (100 μ L), the absorbance at 490 nm was determined using a MultiSkan FC plate reader (Thermo scientific).

Wound Healing Assay. LoVo cells were grown to about 95% confluence in a 6-well plate nearly to confluent cell monolayer. Then a lesion was produced across the cells and washed twice with phosphate-buffered saline (PBS). Following treatment with complex **3a** (0 and 4.0 μ M), the cells were photographed by microscope (magnification, $\times 40$) at 0 and 48h.

General procedure for oxidation of alcohols. To a dry 10 mL round-bottom flask containing alcohol derivatives (2.0 mmol), 6.0 mmol equivalence of hydrogen peroxide(30%) was added. This mixture was then added by the additional 1 mol% of Ru-NHC catalysts and 3 mL acetonitrile. The reaction mixture was stirred at 60°C for 2-5 h. The progress of the reaction was monitored by thin-layer chromatography (TLC). After the completion of the reaction, the solution was cooled to room temperature and the products were purified by flash column chromatography eluting with petroleum ether/ethyl acetate.

X-ray diffraction analysis. Single-crystal X-ray diffraction data of **3a** and **3b** (CCDC 1485263 and 1485264) were collected at 298(2) K on a Siemens Smart-CCD area-detector diffractometer with a Mo-K α radiation ($\lambda = 0.71073$ Å) by using a ω -2 θ scan mode. Unit-cell dimensions were obtained with least-squares refinement. Data collection and reduction were performed using the Oxford Diffraction CrysAlisPro software.^[26] All structures were solved by direct methods, and the non-hydrogen atoms were subjected to anisotropic refinement by full-matrix least squares on F^2 using the SHELXTXL package.^[27] Hydrogen atom positions for all of the structures were calculated and allowed to ride on their respective C atoms with C–H distances of 0.93–0.97 Å and $U_{iso}(H) = -1.2-1.5U_{eq}(C)$.

Acknowledgements

The authors acknowledge supports from the National Natural Science Foundation of Zhejiang Province (LQ14B020003) and the National Natural Science Foundation of China (81571799 and 21202147).

Keywords: N-heterocyclic carbenes • Ruthenium • Pyrazole-functionalized • Anticancer • Catalysis

- a) M. Poyatos, J. A. Mata, E. Peris, *Chem. Rev.* **2009**, 109, 3677-3707; b) N. Marion, S. P. Nolan, *Chem. Rev.* **2009**, 109, 3612-3676; c) F. E. Hahn, M. C. Jahnke, *Angew. Chem. Int. Ed.* **2008**, 47, 3122-3172; d) P. G. Edwards, F. E. Hahn, *Dalton Trans.* **2011**, 40, 10278-10288; e) S. J. Hock, L. A. Schaper, W. A. Herrmann, F. E. Kühn, *Chem. Soc. Rev.* **2013**, 42, 5073-5089; f) L. A. Schaper, S. J. Hock, W. A. Herrmann, F. E. Kühn, *Angew. Chem. Int. Ed.* **2013**, 52, 270-289.
- a) D. Yuan, H. Tang, L. Xiao, H. V. Huynh, *Dalton Trans.* **2011**, 40, 8788-8795; b) S. Zhao, F. Wu, Y. Ma, W. Chen, M. Liu, H. Wu, *Org. Biomol. Chem.* **2016**, 14, 2550-2555; c) C. Mejuto, M. A. García-Eleno, G. Guisado-Barrios, D. Spasyuk, D. Gusev, E. Peris, *Org. Chem. Front.* **2015**, 2, 936-941; d) X. Xie, H. V. Huynh, *Org. Chem. Front.* **2015**, 2, 1598-1603; e) G. Bauer, X. Hu, *Inorg. Chem. Front.* **2016**, 3, 741-765.
- a) T. Simler, P. Braunstein, A. A. Danopoulos, *Chem. Commun.* **2016**, 52, 2717-2720; b) T. Simler, P. Braunstein, A. A. Danopoulos, *Dalton Trans.* **2016**, 45, 5122-5139; c) T. Simler, A. A. Danopoulos, P. Braunstein, *Chem. Commun.* **2015**, 51, 10699-10702; d) B. Vabre, Y. Canac, C. Lepetit, C. Duhayon, R. Chauvin, D. Zargarian, *Chem. Eur. J.* **2015**, 21, 17403-17414.
- a) D. Kim, L. Le, M. J. Drance, K. H. Jensen, K. Bogdanovski, T. N. Cervarich, M. G. Barnard, N. J. Pudalov, S. M. M. Knapp, A. R. Chianese, *Organometallics* **2016**, 35, 982-989; b) Z. Wang, C. Zheng, W. Wang, C. Xu, B. Ji, X. Zhang, *Inorg. Chem.* **2016**, 55, 2157-2164; c) A. Volpe, S. Baldino, C. Tubaro, W. Baratta, M. Basato, C. Graiff, *Eur. J. Inorg. Chem.* **2016**, 2, 247-251.
- a) M. Li, H. Song, B. Wang, *J. Organomet. Chem.* **2016**, 804, 118-122; b) L. Wan, D. Zhang, *Organometallics* **2016**, 35, 138-150; c) A. Rajaraman, A. R. Sahoo, F. Hild, C. Fischmeister, M. Achard and C. Bruneau, *Dalton Trans.* **2015**, 44, 17467-17472.
- a) C. Chen, Q. Xia, H. Qiu, W. Chen, *J. Organomet. Chem.* **2015**, 775, 103-108; b) J. C. Bernhammer, H. V. Huynh, *Organometallics* **2014**, 33, 1266-1275; c) J. C. Bernhammer, H. V. Huynh, *Organometallics* **2014**, 33, 172-180.
- C. G. Hartinger and P. J. Dyson, *Chem. Soc. Rev.* **2009**, 38, 391-401
- B. Rosenberg, L. VanCamp, J. E. Trosko, V. H. Mansour, *Nature* **1969**, 222, 385-386
- W. Liu, R. Gust, *Chem. Soc. Rev.* **2013**, 42, 755-773.
- K. Suntharalingam, S. G. Awuah, P. M. Bruno, T. C. Johnstone, F. Wang, W. Lin, Y. Zheng, J. E. Page, M. T. Hemann, S. J. Lippard, *J. Am. Chem. Soc.* **2015**, 137, 2967-2974.
- a) C. Chen, H. Qiu, W. Chen, *Inorg. Chem.* **2011**, 50, 8671-8678; b) C. Chen, W. Chen, H. Qiu, *Dalton Trans.* **2012**, 41, 13405-13412; c) C. Chen, C. Lu, Q. Zheng, S. Ni, M. Zhang, W. Chen, *Beilstein J. Org. Chem.* **2015**, 11, 1786-1795.
- a) B. Y. Tay, C. Wang, P. H. Phua, L. P. Stubbs, H. V. Huynh, *Dalton Trans.* **2016**, 45, 3558-3563; b) V. Leigh, D. J. Carleton, J. Olguin, H. Mueller-Bunz, L. J. Wright, M. Albrecht, *Inorg. Chem.* **2014**, 53, 8054-8060; c) H. Ohara, W. W. N. O, A. J. Lough, R. H. Morris, *Dalton Trans.* **2012**, 41, 8797-8808; d) L. Mercks, A. Neels, H. Stoeckli-Evans, M. Albrecht, *Inorg. Chem.* **2011**, 50, 8188-8196.
- a) S. Saha, M. Kaur, K. Singh, J. K. Bera, *J. Organomet. Chem.* **2016**, 812, 87-94; b) D. Yang, Y. Tang, H. Song, B. Wang, *Organometallics* **2015**, 34, 2012-2017; c) X. Liu, W. Chen, *Dalton Trans.* **2012**, 41, 599-

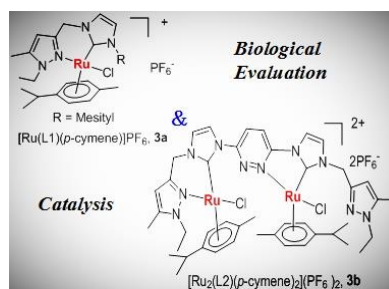
- 608; d) D. Schleicher, A. Tronnier, H. Leopold, H. Borrmann, T. Strassner, *Dalton Trans.* **2016**, 45, 3260–3263; e) W. Ghattas, H. Müller-Bunz, M. Albrecht, *Organometallics* **2010**, 29, 6782–6789.
- [14] X. Liu, W. Chen, *Organometallics* **2012**, 31, 6614–6622; c) J. Ye, X. Zhang, W. Chen, S. Shimada, *Organometallics* **2008**, 27, 4166–4172.
- [15] a) K-M. Lee, J. C.C. Chen, I. J.B. Lin, *J. Organomet. Chem.* **2001**, 617, 364–375; b) U. J. Scheele, S. Dechert, F. Meyer, *Inorg. Chim. Acta.* **2006**, 359, 4891–4900.
- [16] J. Ye, X. Zhang, W. Chen, S. Shimada, *Organometallics* **2008**, 27, 4166–4172.
- [17] a) J. Wimberg, U. J. Scheele, [a] S. Dechert, F. Meyer, *Eur. J. Inorg. Chem.* **2011**, 3340, 3340–3348; b) U. J. Scheele, S. Dechert, F. Meyer, *Chem. Eur. J.* **2008**, 14, 5112–5115.
- [18] a) N. P. Barry, P. J. Sadler, *Chem. Soc. Rev.* **2012**, 41, 3264–3279; b) G. Gasser, I. Ott, N. Metzler-Nolte, *J. Med. Chem.* **2010**, 54, 3–25; c) A. Bergamo, G. Sava, *Dalton Trans.* **2011**, 40, 7817–7823; d) W. H. Ang, A. Casini, G. Sava, P. J. Dyson, *J. Organomet. Chem.* **2011**, 696, 989–998.
- [19] a) J. M. Rademaker-Lakhai, D. Van Den Bongard, D. Pluim, J. H. Beijnen, J. H. M. Schellens, *Clin. Cancer Res.* **2004**, 10, 3717–3727; b) E. Alessio, G. Mestroni, A. Bergamo, G. Sava, *Curr. Top. Med. Chem.* **2004**, 4, 1525–1535; c) C. G. Hartinger, S. Zorbas-Seifried, M. A. Jakupec, B. Kynast, H. Zorbas and B. K. Keppler, *J. Inorg. Biochem.* **2006**, 100, 891–904.
- [20] a) H. Wang, H. Xie, J. Wu, X. Wei, L. Zhou, X. Xu, S. Zheng, *Angew. Chem. Int. Ed.* **2014**, 53, 11532–11537; b) H. Wang, H. Xie, J. Wang, J. Wu, X. Ma, L. Li, X. Wei, Q. Ling, P. Song, L. Zhou, X. Xu, S. Zheng, *Adv. Funct. Mater.* **2015**, 25, 4956–4965; c) H. Xie, X. Xu, J. Chen, L. Li, J. Wang, T. Fang, L. Zhou, H. Wang, S. Zheng, *Chem. Commun.* **2016**, 52, 5601–5604; d) T. Fang, Y. Dong, X. Zhang, K. Xie, L. Lin, H. Wang, *Int. J. Pharmaceut.* **2016**, 512, 39–48; e) J. Wang, H. Wang, J. Li, Z. Liu, H. Xie, X. Wei, D. Lu, R. Zhuang, X. Xu, S. Zheng, *ACS Appl. Mater. & Interfaces.* **2016**, 8, 19228–19237.
- [21] G. Lv, L. Guo, L. Qiu, H. Yang, T. Wang, H. Liu, J. Lin, *Dalton Trans.* **2015**, 44, 7324–7331.
- [22] a) L. Oehninger, M. Stefanopoulou, H. Alborzina J. Schur, S. Ludewig, K. Namikawa, A. Muñoz-Castro, R. W. Köster, K. Baumann, S. Wölfl, W. S. Sheldrick, I. Ott, *Dalton Trans.* **2013**, 42, 1657–1666; b) J-J Zhang, J. K. Muenzner, M. A. A. Maaty, B. Karge, R. Schobert, S. Wölfl, I. Ott, *Dalton Trans.* **2016**, 45, 13161–13168; c) F. Hackenberg, H. Müller-Bunz, R. Smith, W. Streciwilk, X. Zhu, M. Tacke, *Organometallics* **2013**, 32, 5551–5560; d) L. Oehninger, H. Alborzina, S. Ludewig, K. Baumann, S. Wölfl, I. Ott, *ChemMedChem* **2011**, 6, 2142–2145.
- [23] a) I. Song, N. Savaraj, Z. H. Siddik, P. Liu, Y. Wei, C. Wu, M. T. Kuo, *Mol. Cancer. Ther.* **2004**, 3, 1543–1549; b) S. Fu, A. Naing, C. Fu, M. T. Kuo, R. Kurzrock, *Mol. Cancer. Ther.* **2012**, 11, 1221–1225.
- [24] a) A. R. Naziruddin, C. Zhuang, W. Lin, W. Hwang, *Dalton Trans.* **2014**, 43, 5335–5342; b) D. Gnanamgari, E. L. O. Sauer, N. D. Schley, C. Butler, Christopher D. Incarvito, R. H. Crabtree, *Organometallics* **2009**, 28, 321–325; c) Z. Şahin, N. Gürbüz, İ. Özdemir, O. Şahin, O. Büyükgüngör, M. Achard, C. Bruneau, *Organometallics* **2015**, 34, 2296–2304; d) F. E. Fernández, M. C. Puerta, P. Valerga, *Organometallics* **2012**, 31, 6868–6879; e) W. W. N. O, A. J. Lough, R. H. Morris, *Organometallics* **2011**, 30, 1236–1252; f) S. K. Gupta, S. K. Sahoo, J. Choudhury, *Organometallics* **2016**, 35, 2462–2466.
- [25] S. S. Kadam, L. Maie, I. Kostakis, N. Pouli, J. Tousek, M. Necas, P. Marakos, R. Marek, *Eur. J. Org. Chem.* **2013**, 30, 6811–6822.
- [26] *CrysAlisPro*, Oxford Diffraction Ltd, Oxford, UK, **2008**.
- [27] G. M. Sheldrick, *SHELXS-97 and SHELXL-97, Program for X-ray Crystal Structure Refinement*, University of Göttingen, Göttingen, Germany, **1997**.

Entry for the Table of Contents (Please choose one layout)

Layout 1:

FULL PAPER

Two pyrazole-functionalized N-heterocyclic carbenes (NHCs) were prepared and characterized. In vitro results showed that complex **3a** had comparable cytotoxicity with clinically approved cisplatin. More impressively, complex **3a** evoked significant death of cisplatin-resistant gastric cancer SCG7901-R cells. In addition, both ruthenium-NHC complexes were demonstrated to be efficient catalysts for the oxidation of various alcohols.



Pyrazole-Functionalized NHC-Ru(II)

Chao Chen,* Shengliang Ni, Qing Zheng, Meifang Yu and Hangxiang Wang*

Page No. – Page No.

Synthesis, Structure, Biological Evaluation and Catalysis of Two Pyrazole-Functionalized NHC-Ru(II) Complexes

* N-heterocyclic carbenes

Accepted Manuscript